Shanmugam Palanisamy* and Börje S. Gevert

Hydrodeoxygenation of fatty acid methyl ester in gas oil blend–NiMoS/alumina catalyst

https://doi.org/10.1515/gps-2016-0117
Received August 19, 2016; accepted August 28, 2017; previously published online October 6, 2017

Abstract: Hydrotreating of 10% fatty acid methyl ester (FAME) blended in gas oil was carried out by an NiMo-S/alumina catalyst and performed at an elevated temperature (300–400°C), a space velocity of 0.7–1.5 1/h and pressure 5 MPa. The gas oil was a straight run North Sea crude oil containing 295 ppm sulfur content which was desulfurized in a hydrotreating upgrading process. The physicochemical properties following hydroprocessing of FAME showed that sulfur content was reduced to 3 ppmw, with an increase in aromatic content and cloud point. It was confirmed that decarboxylation depends on temperature and space velocity and decarbonylation depends on temperature, but not on space velocity of feed. High sulfur content in the feedstock supports slow deactivation of the catalyst and low coke formation.

Keywords: deactivation and NiMoS catalyst; decarbonylation; decarboxylation; decomposition; FAME; gas oil; hydrodeoxygenation.

1 Introduction

Consumption of conventional diesel for transportation increases continuously with economic growth and globalization. Stringent legislative law, which applies to EU countries, has put an emphasis on the importance of decreasing the use of conventional fuels that contribute to the greenhouse effect [1–4]. Renewable fuels (such as fatty acid methyl ester [FAME], rapeseed methyl ester, and dimethyl ether) may be viable alternatives, and several pilot plant studies to develop an effective use of biomass have been reported in the literature [4–9]. It has been shown that refineries can be adapted to replace crude oil with renewable feeds. Traditional refining processes like hydrotreatment and hydrodesulfurization (HDS), that are well established to upgrade middle distillates [7, 10, 11], can also be used for upgrading renewable feedstocks. One such process in practice is hydrodeoxygenation, which is removal of oxygen by hydrogenolysis [12–17]. Decarbonylation or decarboxylation of FAME produces C_{17} (undesired product) by removal of a carbonyl group as CO or CO_2 from the ester group.

It has been found that bimetallic catalysts (e.g. NiMo) have a higher conversion rate in the hydrotreating process compared to monometallic catalysts [13, 18, 19]. For instance $NiMoS/Al_2O_3$ and $CoMoS/Al_2O_3$ catalysts are used to produce C_{18} and C_{17} hydrocarbons of high yield from hydrotreating FAME or rapeseed oil with reducing agents such as H_2 or H donors [10, 20, 21]. As the sulfur content is generally low in biofuels (<0.002 wt%), addition of a sulfiding agent is required to maintain the activity of the catalyst [22]. This can be solved by using sulfur-rich feedstocks or by the addition of a sulfur compound as a substitute to FAME [11, 16]. Senol et al. [23] and Viljava et al. [24] observed that use of H_2S as a substitute has no effect in the selectivity of alcohol and ester hydrogenation, however, the reaction stability of the HDS catalysts was improved. Furthermore, studies have shown that H_2S and water substitution increase the rate of intermediate species formation on both Co and $Ni\text{-}MoS/Al_2O_3$ catalysts [25–29]. Promoting the catalyst with Ni increased the activity and stability as compared to using Co as a catalyst promoter [3, 27–29]. Overview of the studies implies the effectiveness of renewable feedstock on the catalytic process. To increase the understanding of thermal treatment with middle distillates and FAME, further studies in pilot scale are needed. In this research work, $NiMoS/Al_2O_3$ was used to study the light gas oil (LGO) upgrading in the presence or absence of FAME with a reducing agent (H_2). High sulfur content in LGO was used to investigate catalyst performance and deactivation properties. In particular, the aromatic content, cloud point and distillate fractions of the hydrogenated products are in focus. For the catalytic process, temperature and space velocity were the most important parameters to attain a better optimization for the upgrading system.

2 Materials and methods

2.1 Feed material

The refined FAME feedstock was supplied by Preem AB (Göteborg, Sweden), which contains fatty esters and acids with traces of neutrals

***Corresponding author: Shanmugam Palanisamy,** Department of Chemical Engineering, Kongu Engineering College (Autonomous), Erode 638060, India, e-mail: shapal.chem@kongu.edu
Börje S. Gevert: Kempross AB, Larserds Lyckor 14, 425 39 Hisings Kärra, Sweden

and resin acids. The FAME feedstock contains: octadecadienoic acid C_{18}:2 (1.6 wt%), octadecenoic acid C_{18}:1 (1.0 wt%), octadecanoic acid C_{18}:0 (0.4 wt%), methyl palmitate (3.6 wt%), methyl linolenate (8.6 wt%), methyl linoleate (45.6 wt%), methyl oleate (20.7 wt%) and other esters (17.9 wt%).

LGO was the diesel fraction supplied by Preem AB. The LGO had 17.6 (v/v%) aromatics, 295 (ppmw) sulfur and C_8 to C_{16} hydrocarbon fractions [22]. Table 1 provides the physicochemical properties of the LGO.

2.2 Hydroprocessing experiments

The Trilobe HDN-60 (NiMo/γ-Al_2O_3) catalyst (Criterion Catalysts, Farehem, UK), consisting of Ni-Mo/γ-Al_2O_3 with 2.5–3% Ni, 12.5–13.5% Mo and 83–85% γ-Al_2O_3, was used for the experiments [22]. The catalyst consisted of 1/32-in extrudes (calcined at 400°C overnight) and 31 ml (27.43 g) was loaded in the fixed-bed reactor at the middle section for in-site sulfidation before the hydroprocessing experiment. The catalyst surface properties are presented in Table 2. Sulfidation of the catalyst was carried out at 400°C and achieved by introducing H_2S (10 v/v% sulfur in H_2) at 200 mln/min for 3 h to the catalyst and kept overnight under N_2 presence [22]. After sulfidation of the catalyst, pure LGO was fed for 10 days at 360°C and 5 MPa in order to achieve a stabilized coke deposition on the catalyst surface, enabling stable activity during the experiments [30].

The experimental set-up consisted of a feed tank, pump, trickle-bed reactor, separator tank, gas flow meter and product collector [22, 30]. Both sides of the reactor were fastened with heavy bolts to a thickness of 19.3 mm, which were connected with inlet and outlet pipes. The down flow fixed-bed reactor, insulated with three independent heating zones, had an internal diameter of 1.8 cm; the void space above and below the catalyst bed was filled with borosilicate

Table 1: Properties of a fresh (before activation) and spent (after treatment) catalyst determined by N_2 sorption using the BET method.

Material	Specific surface area (m^2/g)	Pore size (nm)[a]	Pore size (nm)[b]	Pore volume (cm^3/g)[a]	Pore volume (cm^3/g)[b]	Coke formation (db, w/w)[c]
Fresh NiMo	156.300	8.330	6.950	0.314	0.311	<0.09
Spent NiMo	54.500	6.960	5.110	0.117	0.124	4.8

[a]Calculated from the adsorption branch of the N_2 sorption isotherm using the BJH method.
[b]Calculated from the desorption branch of the N_2 sorption isotherm using the BJH method.
[c]Analyzed by Karlshamn Kraft AB, ASTM D 5291 standard test method.
db, dry basis; BET, Brunauer–Emmett–Teller; BJH, Barrett-Joyner-Halenda.

Table 2: Physicochemical properties of hydroprocessed light gas oil (LGO) at 5 MPa pressure.

Parameters	Feed[a]	LHSV (1/h)						Gas oil grade[b]	Reference test method
		0.35	0.5	0.75	1	1.2	1.5		
Compositions									
LGO recovery (wt%)		80	84	91	93	95	96		
Cracked (wt%)		<10	<10	7	5	4	3		
Aromatic content (%v/v)	17.8	16.2	17.3	17.3	17.6	17.9	17.9	≤5[c]	SS 155116:1993
Distillation									
Dist: temperature at IBP (°C)	196	205	198	194	199	200	205	≥180	*ASTM D86*
Dist: temperature at 10% v/v rec. (°C)	211	213	210	209	209	211	214		*ASTM D86*
Dist: temperature at 50% v/v rec. (°C)	231	229	229	229	229	230	230		*ASTM D86*
Dist: temperature at 90% v/v rec. (°C)	250	248	248	249	249	248	250		*ASTM D86*
Dist: temperature at 95% v/v rec. (°C)	257	255	256	256	256	256	257	≤295	*ASTM D86*
Dist: FBP (°C)	271	271	271	270	268	268	268		*ASTM D86*
Dist: recovery (%)	98.1	98	98	98.2	98.5	98.1	98.1		*ASTM D86*
Others properties									
Sulfur content (ppmw)	295	3	1	3	8	26	17	≤10[b]	*ASTM D5453-00*
Nitrogen content (ppmw)	<1	<1	<1	<1	<1	<1	<1		*ASTM D4629-08*
Density at 15°C (kg/m^3)	823	816	818	819	818	820	819	807–817	*ASTM D4052-09*
Viscosity at 40°C (mm^2/s)	1773	1772	1765	1757	1750	1773	1795	1500–3800	*ASTM D 7042-04*
Cloud point (°C)	−40	−40	−40	−40	−39	−41	−40	−22[d]	*ASTM D2500-05*

[a]LGO extracted from crude oil distillation (Preem AB, Sweden).
[b]Swedish Environmental Class (EC1) gas oil grade.
[c]Polyaromatic hydrocarbon (PAH) (tri+) should be less than 0.02%. Test reference: IP 391/95. Feed LGO contains PAH = 0.64%.
[d]Minimum requirement for winter climate.
FBP, final boiling point; IBP, initial boiling point; LGO, light gas oil; LHSV, liquid hourly space velocity.

glass pellets with a diameter of 2 mm. The reciprocal dossier pump was used to pump liquid feed with H_2 gas in co-current flow. Products were withdrawn periodically from the separator tank. The reaction conditions were controlled through a proportional-integral-derivative controller and products were taken subject to the manual time control at ambient conditions [30].

2.3 Distillation and analysis

The product was collected at 20 h intervals, and subsequently placed in the distillation reboiler in N_2 atmosphere [30]. A 2 l reboiler in a simple distillation column operates at a desirable cut-off temperature of 162°C; water and lighter hydrocarbons were separated from products and precaution was taken not to loss middle distillates [22, 30]. The distillate containing lighter hydrocarbons and water was condensed through a water cooler (to keep the losses low). Between 90 and 99 vol% gas oil was recovered (as shown in Figure 1) from the residue and analyzed with respect to properties of the upgraded products.

The upgraded product before and after distillation was analyzed using a gas chromatograph (GC) technique. Simulated distillation (ASTM D2887) was performed using a GC technique (Varian 3400, Agilent Technologies, CA, USA) equipped with a packed column (10% silicon OV-101, 80–100 mesh, 1 m × 3.175 mm × 2.00 mm) and a flame ionization detector (FID). The injector and detector were maintained at 300°C and the initial column temperature was maintained at 40°C and heated to 325°C (18°C/min). Finally the temperature was maintained at 325°C for 10 min. A Varian 4270 integrator was used for data computation.

The fuel gas collected from the top outlet of the separating tank was analyzed using the Clarus 500 online GC (Perkin Elmer, MA, USA). This GC had a thermal conductivity detector (maintained at 200°C with oven heat-up of 40–60°C at 2°C/min in helium gas) and FID detectors (maintained at 60°C in nitrogen gas), and four valves actuated by nitrogen gas at 0.4 MPa and connected with 600 link switch controllers that interpret signal to integrator [22, 30]. The specified detectors were a thermal conductivity detector to analyze CO, CO_2 and CH_4 and lighter hydrocarbon fractions were analyzed in an FID.

The physicochemical properties of the residue were analyzed at Preem refinery in Göteborg, Sweden. The spent catalyst was purified by extracting the feed solvent (LGO) with m-xylene for more than 22 h and washing in a Sohxlet apparatus. The washed catalyst was dried at 120°C in nitrogen atmosphere and the degree of coke deposition was analyzed at Karlshamn Kraft AB (Karlshamn, Sweden) using an ASTM D 5291 standard test method.

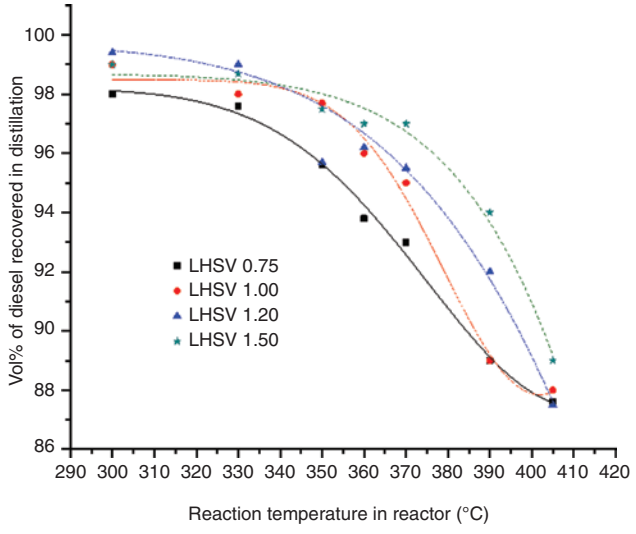

Figure 1: Volume % of gas oil recovered from the product by simple distillation on a cut point temperature 162°C. The distillate contains water and naphtha fractions (majority are C_5 to C_{12} and traces of C_{13} to C_{16} hydrocarbons).

3 Results and discussion

This work focuses on upgrading of LGO in the presence and absence of FAME over a NiMoS/γ-Al_2O_3 catalyst. In the experiments, the reactor pressure (5 MPa) and the feed of 10 wt% FAME in LGO (10%F) were kept constant. Parameters that varied were H_2 flow/10%F, reactor temperature and liquid hourly space velocity (LHSV: 31 ml/h feed pumped in 31 ml reactor volume equals 1 l/h). Standard reaction conditions referred to in literature were used, i.e. 360°C and 5.0 MPa [18, 20].

The error tolerance in mass balances calculation for lighter hydrocarbons and middle distillate fractions was approximately 0.5–1 wt%. In addition, traces of heavy hydrocarbons beyond C_{17} are considered to be negligible. The main components in the residue are hydrocarbons from nonane hydrocarbons to heavy hydrocarbons ($\leq C_{18}$) with traces of lighter hydrocarbons.

3.1 HDS reaction

In order to remove sulfur from the LGO feed, an NiMoS/γ-Al_2O_3 catalyst was used for the HDS reaction forming H_2S. The reaction was run at 360°C [7, 10, 11], and the LGO space velocity variation resulted in varying physicochemical properties of the products. The desired properties for LGO are aromatic composition with polyaromatic hydrocarbon (PAH), distinguished distillate recovery on boiling point and other properties (e.g. sulfur and nitrogen content, density, viscosity and cloud point) in accordance with ASTM standard (Table 3). The boiling point of the product was in the range of the LGO standard grade, i.e. between 180°C and 289°C. The aromatic content of the LGO feed was 17.8 v/v%, however, when the space velocity was increased from 0.4 1/h to 1.5 1/h, the aromatic content varied from about 16.2 v/v% to 17.9 v/v%, which is much

Table 3: Physicochemical properties of the product from 10% fatty acid methyl ester (FAME) + light gas oil (LGO) by Ni-Mo catalyst for varied temperatures and a feed space velocity at 5 MPa pressure.

Parameters	LHSV at To = 360°C				To (°C) at LHSV = 1					Reference test method
	0.75	1	1.2	1.5	390	370	350	330	300	
Compositions										
Product/feed (%)	90.3	92.8	95.8	96.6	89	90.6	93	95.6	98	
Aromatic (mo-, di-) (%v/v)	16	17.7	17.6	17.4	22.8	18.9	17.2	15.9	16.9	SS 155116:1993
PAH (tri+) (%v/v)	0.64	0.54	0.3	0.36	1.00	0.55	0.40	0.42	0.32	
Liquid fraction (wt%)										
$>\Sigma C_6$	1.2	0.9	0.6	0.5	2.1	0.9	1.0	1.8	0.5	
C_6–C_9	5.0	4.4	7.3	7.0	6.4	4.4	2.2	1.9	1.6	
C_{10}–C_{14}	77.6	78.6	73.1	75.2	65.7	71	73.4	72.4	70.7	
ΣC_{15}	3.5	6.3	8.5	7.5	7.7	6.1	7.0	6.5	8.6	
ΣC_{16}	2.4	2.6	2.5	1.8	9.8	9.0	9.3	8.5	8.5	
ΣC_{17}	5.0	3.6	3.5	3.1	5.9	5.0	3.7	4.1	4.0	
ΣC_{18}	5.0	4.5	4.3	4.1	2.2	3.4	3.0	4.2	5.3	
Heavy fraction	0.3	0.4	0.7	0.9	0.2	0.2	0.5	0.6	0.6	
Distillation										
Dist: temperature at IBP (°C)	204	213	208	208	191	207	204	212	207	*ASTM D86*
Dist: temperature at 10% v/v rec. (°C)	208	220	217	216	208	214	214	219	215	*ASTM D86*
Dist: temperature at 50% v/v rec. (°C)	215	237	233	235	235	235	235	236	236	*ASTM D86*
Dist: temperature at 65% v/v rec. (°C)	235	244	243	244	245	242	242	243	245	*ASTM D86*
Dist: temperature at 90% v/v rec. (°C)	265	265	269	266	269	265	263	267	270	*ASTM D86*
Dist: temperature at 95% v/v rec. (°C)	283	284	288	285	283	284	281	286	289	*ASTM D86*
Others properties										
Cloud point	−19	−18	−17	−16	−24	−20	−18	−15	−14	*ASTM D2500-05*
Sulfur content (ppmw)	2	7	9	4	5	3	2	1	4	*ASTM D5453-00*
Nitrogen content (ppmw)	<1	<1	<1	<1	<1	<1	<1	<1	<1	*ASTM D4629-08*
Density at 15°C (kg/m^3)	819	822	820	820	825	822	820	820	821	*ASTM D4052-09*
Viscosity at 40°C (mm^2/s)	1907	1973	1924	1918	1842	1902	1912	1982	1990	*ASTM D 7042-04*

IBP, initial boiling point; LHSV, liquid hourly space velocity; PAH, polyaromatic hydrocarbon.

higher than the LGO grade standard of ≤5 v/v%. The cloud point, density and viscosity were in the same range as the LGO standard grade. The sulfur content was reduced from 295 ppmw to less than 27 ppmw. However, the sulfur content in the upgraded product was strongly influenced by the LHSV. For instance at an LHSV of 0.5, the sulfur level was 1 ppmw, while increase in space velocity caused an increase in sulfur content in the product. Space velocities around 0.35–0.5 1/h result in high cracking, which leads to high yields of petroleum gas and naphtha with a distillate range below 170°C. Thus, the operating range of LHSV was considered between 0.75 and 1.5 for further results in orientation and discussion.

3.2 Co-processing FAME and LGO

LGO with 10% FAME (10%F) was co-processed using the experimental parameters as mentioned previously. When mixing FAME (feed) and LGO, a slight precipitation was observed that was dissolved by warming, without loss of feedstock. The analytical results of the upgraded products at elevated temperature and LHSV are shown in Table 3. We examined the conversion, selectivity and yield, such that:

$$\text{Conversion} = \frac{\text{convertedfeed} \times 100}{\text{suppliedfeed}},$$

$$\text{Selectivity} = \frac{\text{desiredproduct}}{\text{undesiredproduct}},$$

$$\text{Yield} = \frac{\text{desiredproduct} \times 100}{\text{suppliedfeed}}$$

Upon deoxygenation of FAME, the desired product is C_{18}, in order to obtain a high cetane number of upgraded LGO. The formation of C_{18} during upgrading of 10%F decreased for increasing LHSV and temperature, from 5 wt% to 4 wt% (concentration in the product) at elevated LHSV (0.75–1.5) and 5–2 wt% for elevated temperature (300–390°C) (Table 3). This formation was 5 wt% to 3 wt%

and 4 wt% to 6 wt% for elevated LHSV and temperature, respectively. For different H_2/10%F ratios, there are no variations in viscosity, density or aromatic properties, except for a slight decrease in the naphtha concentration from 2.1 wt% to 1.6 wt% for increasing H_2/10%F ratios (Table 4).

CO and CO_2 are mainly formed when a carbonyl group is detached from the carbon chains of FAME, as the C=O bond is stronger than the C-C and C-H bonds, which is due to configuration stability [2, 18]. The degree of carbonyl detachment in the upgrading reaction can hence be followed in the product formation (as CO and CO_2). Consequently, H-β scission by thermal decomposition leads to formation of carbocations in paraffin chains [29, 30]. Hydrogen redistribution in paraffin chains has a tendency to further inhibit H-β scission in forming smaller carbonium ion groups, such as lighter hydrocarbons of low boiling chemical species.

Deoxygenation and decarbonylation reactions, that involve partial cracking, mainly occur at the surface and in the pores of the catalyst [22–26]. This is confirmed by the decrease in naphtha concentration as the H_2 content was increased, for constant LHSV. The aromatic content did not change upon varying the H_2 ratio owing to the equilibrium between dehydrogenation and hydrogenation, which was mainly dependent on temperature. The C=C reactivity in large molecules in FAME, such as methyl linoleate and methyl linolenate, depend on the type and position of the fatty acid component in the molecule. Thus, mainly linoleic and oleate compounds undergo cracking at the C=C bond position via carbonium ion scission (at mass transfer limitation) [2]. However, the C-(CO) (α-bond) bond will likely break more easily than the C=C bond in unsaturated hydrocarbon chains, whereas at higher temperatures the C=C bonds (e.g. C=C bonds 9 or 12 in methyl oleate) will likely break in monounsaturated compounds [2, 30]. Similarly, decomposition and H-β scission have both been observed for C-C and C-H bonds, which have the same endothermicity. Hence, Osmont et al. [2] suggest that the two reaction pathways in cracking (i.e. decarbonylation and decarboxylation) are equally probable for initiating the process [23, 31–33]. The thermal decomposition of FAME, occurring around 350°C, could for example be α bond breaking resulting in C_{17}. The probability for cracking to occur at the bond of the seventh position and ninth position is generally low because of the weak pi-bonding over acidic sites or on alumina [30, 34, 35].

The aromatic content in the product increases steadily for the studied temperature from 16 v/v% to 18 v/v%. In particular, for temperatures above T = 350°C, the aromatic content in the product increases (from 17 v/v% to 22.8 v/v%) as can be seen in Table 3, which is above the thermodynamic equilibrium. The feed (10%F) contains 0.58 v/v% PAH, which is higher than the standard limit which should be less than 0.02 v/v% in conventional Swedish diesel. Yet, as shown in Table 3, the PAH content in the product increases from 0.32 v/v% to 0.55 v/v%, for temperatures between 300°C and 370°C. The shorter residence time (higher LHSV) reduces the diaromatic or PAH (from 0.64 v/v% to 0.36 v/v%) but increases the monoaromatic content. By varying the H_2 partial pressure in the system, the PAH formation was unchanged in products (Table 4). Change in H_2 resulted in increased PAH (0.98 v/v%). These results indicate that an increasing temperature and a decreasing space velocity cause an increase in PAH and a reduction in monoaromatic and diaromatic compounds (Table 3). Therefore, it is important to identify the optimum conditions for this process, e.g. altering the dehydrogenation mechanism by decreasing the H_2 concentration in the feed, as the H_2 content directly influences the aromatization. Moreover, the presence of monoaromatic compounds in the feed requires a high residence time over the catalyst sites in order to undergo a de-aromatization reaction within the hydrogenation conditions used in the present study.

Table 4: Physicochemical properties of 10% fatty acid methyl ester (FAME) + light gas oil (LGO) product obtained by hydrodesulfurization (HDS) on Ni-Mo catalyst for different H_2 input at liquid hourly space velocity (LHSV) = 1 1/h and T = 360°C.

Parameters	Hydrogen / Feed (10% FAME LGO) (v/v)		
	60	90	150
Naphtha (wt%)	2.1	1.8	1.6
Diesel fraction (wt%)	91	91	91
ΣC_{17} (wt%)	3.3	2.9	3.2
ΣC_{18} (wt%)	3.0	3.3	3.1
Rest (wt%)	0.6	1.0	1.1
Aromatic content (%v/v)	22.7	23.0	23.0
PAH (tri+) (%v/v)	0.96	0.98	0.94
Sulfur content (ppmw)	32	27	28
Cloud point (°C)	−21	−20	−21

PAH, polyaromatic hydrocarbon.

3.3 Catalyst deactivation

Generally, the sulfur content in the upgraded product is less than 10 ppmw (Figure 2). Initially, a few product samples contained about 25 ppmw sulfur and after some time on stream, the samples showed less than 10 ppmw of sulfur. The explanation may be that the active sites have

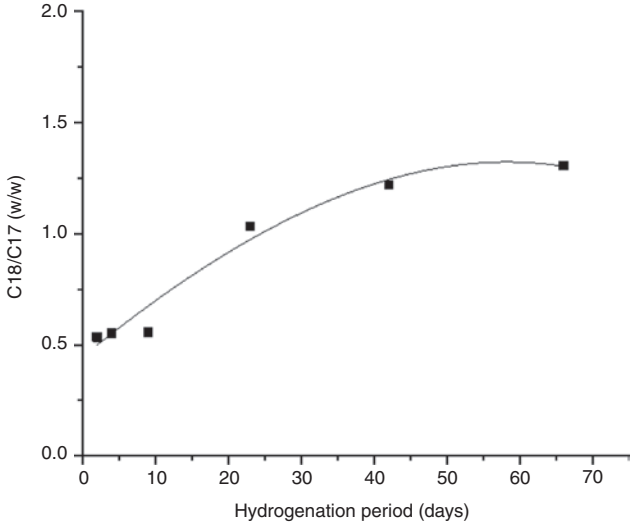

Figure 2: C_{18}/C_{17} ratio versus hydrogenation period of 10% fatty acid methyl ester (FAME) with light gas oil (LGO) at 360°C with liquid hourly space velocity (LHSV) = 1 1/h and P = 5 MPa.

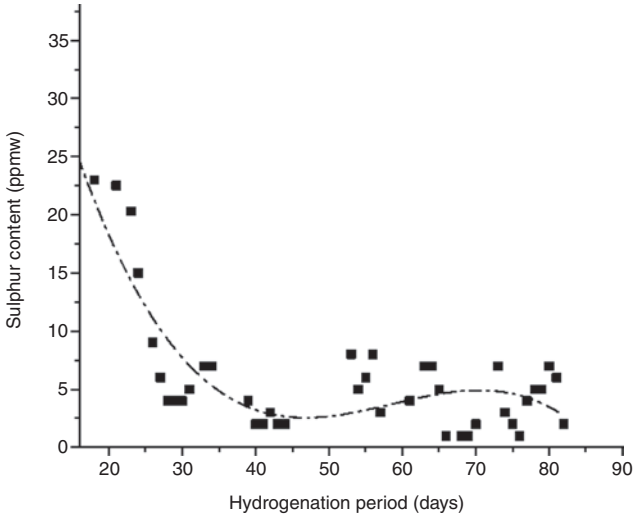

Figure 3: Amount of sulfur content versus hydroprocessed 10% fatty acid methyl ester (FAME) in light gas oil (LGO) for all conditions.

a weak Fermi level over transition metals [35], which prevailed to form H_2S by excess hydrogen. The vacant sites that are replaced by sulfur atoms have a high reaction rate for H_2S formation with adjacent H-donor, however this is dependent on the interfacial mass transfer on the catalytic surface [36]. Thus, continuous addition of sulfur on vacant sites significantly lowers the deactivation of the catalyst [36]. Preferably, branched cyclic compounds in the LGO fraction had steric hindrances; desulfurization of the reaction rate reduced by hindrance of presences of adjacent S atoms near to the alkyl group, for instance alkyl-benzo thiophene, in middle distillate. This scission determines the reaction rate over the active sites at the surface [37].

Table 2 shows the porosity and surface area of a fresh catalyst (fresh NiMo) and a hydrotreated spent catalyst (spent NiMo). The pore volume of the fresh and spent NiMo catalysts is 0.31 cm^3/g and 0.12 cm^3/g, respectively. Similarly, the surface area is 156 m^2/g and 54 m^2/g for fresh and spent NiMo catalysts, respectively. The pore plugging and diminishing surface area are indications of coke deposition. The selectivity of the product measured as the C_{18}/C_{17} ratio is 0.5 over the fresh catalyst, while after an extended period of reactor run, this ratio increased to 1.3 (Figure 3). This low ratio may be due to domination of the decarboxylation/decarbonylation reaction route as compared to a deoxygenation reaction pathway, in both pores and on the surface of the catalyst. Here, a major part of the decomposition product indicates that the active sites were blocked by coke formation in the pores. The selectivity towards the upgraded products is mainly determined by the catalyst structure [38] and the reaction conditions. Thus, -Mo-S- on the surface contributes highly to the deoxygenation reaction compared to other types of promoters [39]. The presence of sulfur and H_2 induces a higher degree of deoxygenation, which tends to increase the C_{18} presence in the product. The FAME deoxygenation on support material, γ-Al_2O_3, has acid sites, and its ability to induce cracking of hydrocarbon on the surface and pores is comparatively higher than in Mo active sites [39]. The sulfur content in the product varies between 1 ppmw and 8 ppmw for all samples measured (Table 2), suggesting that there is low deactivation over the catalyst. By contrast, high PAH (0.64 v/v% in feed LGO) from the feed has a tendency to increase the coke formation in the pores, which is in agreement with previous results [40].

3.4 Lighter hydrocarbon

For C_{18} formation, the ester group is the most active for hydrogenation of the carboxylic acid group, indicating that the hydrogenation reaction occurs through the carboxyl group following the route via the aldehyde group forming alcohol and, finally dehydration to form C_{18}. Methane is the main gas product that detached from the ester group. Furthermore, there is evidence for CO_2 and CO formation (Figure 4). Here, as the temperature increases, formation of CO by decarbonylation is between 0.2 wt% and 2.5 wt%, with a simultaneous increase of CO_2 in the gas phase, although marginally from 0.1 wt% to 0.3 wt%. Decarbonylation is predominantly higher than decarboxylation during thermal decomposition. This thermal effect on the bond scission of H_3C-O is energetically

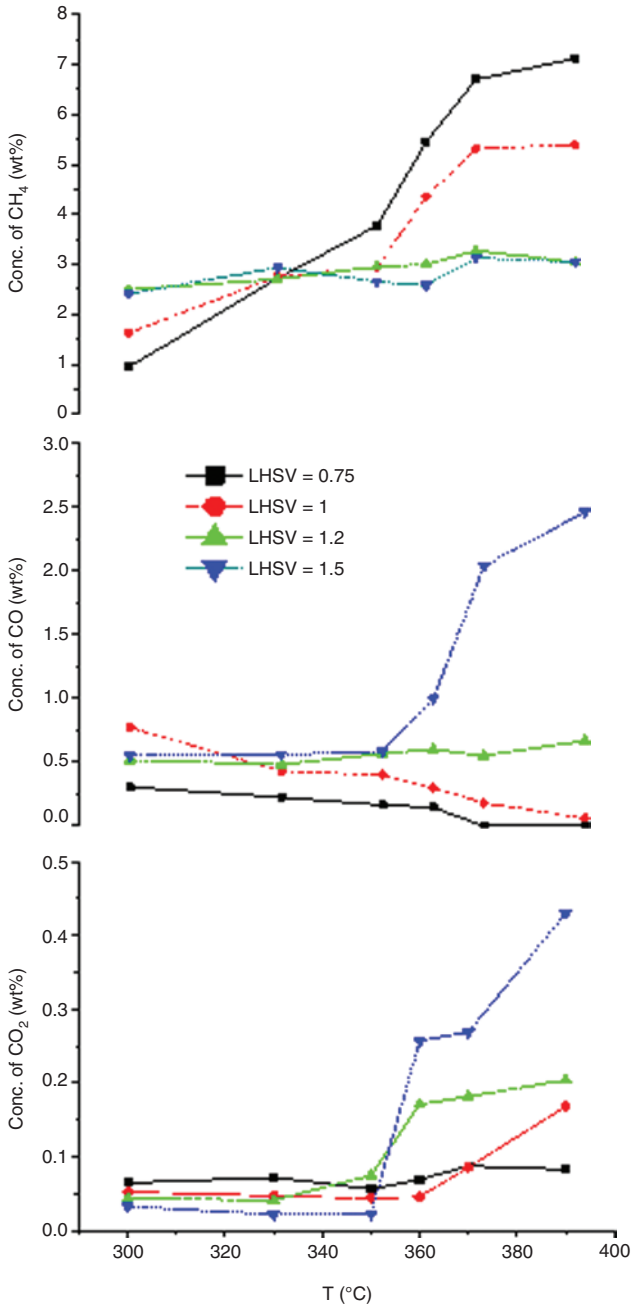

Figure 4: CO, CO_2 and CH_4 concentration in the gas outlet with elevated temperature and space velocity at 5 MPa pressure. Here, liquid hourly space velocity (LHSV) was ■ 0.7, ● 1.0, ▲ 1.2 and ▼ 1.5.

favored over the O-(CO) bond [2, 30, 41]. Thus, both the H_3C-O* and *O-(CO) radicals form alcohol; further alcohol dehydrated into water and hydrocarbon. In the case of the *O-(CO) radical, decomposition occurs by α-bond cleavage, which leads to formation of CO and C_{17} compounds. Figure 4 depicts high methane formation at low space velocity and relatively high temperatures. With high hydrogen partial pressure in the reactor, methanation possibly occurs, as CO disproportionation reaction produces C radicals and forms methane. Dissociation of CO is a rate-determining step of methanation [42], hence the activation energy of the hydrogenation rate increases at low space velocity. We found that it is not viable to form CO from CO_2 in the methanation process, whereas, only CO hydrogenation favors high methane formation. The results indicate that the decarbonylation depends only on temperature and there is no effect by space velocity of feed, whereas decarboxylation depends on both temperature and space velocity.

4 Conclusion

From the above discussion, we conclude that:

- Decarbonylation only depends on temperature, whereas decarboxylation depends on elevated temperature and space velocity.
- There is no FAME presence in the final upgraded product.
- The sulfur content of the upgraded product can achieve up to 1–3 ppmw. The variation of product selectivity observed was mainly by coke formation.
- Aromatic content increases with temperature; in particular, PAH results in an up-swing for higher temperature.
- The optimal condition depends on C_{18} and C_{17} formation and cloud point. Further, aromatic content has some influence on the selection of conditions.

Acknowledgments: We would like to thank Preem AB, Sweden for the financial and feedstock support. Special thanks to Manuel Forner Durá and Estela Garcia for experimental support.

Conflict of interest statement: The authors declare to have no conflicts of interest regarding this article.

References

[1] Zabaniotou A, Ioannidou O, Skoulou V. *Fuel* 2008, 87, 1492–1502.
[2] Osmont A, Yahyaoui M, Catoire L, Gokalp I, Swihart MT. *Combust. Flame* 2008, 155, 334–342.
[3] Senol OI, Viljava TR, Krause AOI. *Catal. Today* 2005, 100, 331–335.
[4] Demirbas A. *Energy Combust. Sci.* 2007, 33, 1–18.
[5] Thuijl EV, Ross CJ, Beurskens LWM. Available at: www.ecn.nl/docs/library/report/2003/c03008.pdf, 2003.

[6] Naik SN, Goud VV, Rout PK, Dalai AK. *Renew. Sust. Energ. Rev.* 2010, 14, 578–597.
[7] Pawelec B, Navarro RM, Campos-Martin JM, Fierro JLG. *Catal. Sci. Technol*. 2011, 1, 23–43.
[8] Shahbazali E. *Green Process. Synth*. 2013, 2, 87–88.
[9] Simacek P, Kubika D, Sebor G, Pospisil M. *Fuel* 2010, 89, 611–615.
[10] Murti SDS, Choi KH, Sakanishi K, Okuma O, Korai Y, Mochida I. *Fuel* 2005, 84, 135–142.
[11] Chisholm MH. *Polyhedron* 1997, 16, 3071.
[12] Donnis B, Egeberg RG, Blom P, Knudsen KG. *Top. Catal.* 2009, 52, 229–240.
[13] Yakovlev VA, Khromova SA, Sherstyuk OV, Dundich VO, Ermakov DY, Novopashina VM, Lebedev MY, Bulavchenko O, Parmon VN. *Catal. Today* 2009, 144, 362–366.
[14] Serrano-Ruiz JC, Dumesic JA. *Energy Environ. Sci*. 2011, 4, 83–99.
[15] Speight JG. *Handbook of Petroleum Product Analysis*, John Wiley & Sons: New Jersey (USA), 2002, pp. 56–60.
[16] Tiwari R, Rana BS, Kumar R, Verma D, Kumar R, Joshi RK, Garg MO, Sinha AK. *Catal. Commun.* 2011, 12, 559–562.
[17] Palanisamy S, Gevert BS, World Renewable Energy Congress (2011), 8–13, May 2011 Sweden, BE01, 057:073, 546–551.
[18] Kubicka D, Kaluza L. *Appl. Catal., A* 2010, 372, 199–208.
[19] Bihan LL, Yoshimura Y. *Fuel* 2002, 81, 491–494.
[20] Senol OI, Viljava TR, Krause AOI. *Catal. Today*, 2005, 106, 186–189.
[21] de Paulo AA, da Costa RS, Rahde SB, Vecchia FD, Seferin M, dos Santos CA. *Appl. Therm. Eng*. 2016, 98, 288–297.
[22] Palanisamy S, Gevert BS. *Fuel Process. Technol.* 2014, 126, 435–440.
[23] Senol OI, Ryymin EM, Viljava TR, Krause AOI. *J. Mol. Catal. A Chem.* 2007, 268, 1–8.
[24] Viljava TR, Komulainen RS, Krause AOI. *Catal. Today* 2000, 60, 83–92.
[25] Senol OI, Viljava TR, Krause AOI. *Appl. Catal. A* 2007, 326, 236–244.
[26] Senol OI, Ryymin EM, Viljava TR, Krause AOI. *J. Mol. Catal. A Chem.* 2007, 277, 107–112.
[27] Badilla-Ohlbaum R, Chadwick D, Gavin DG. *Fuel* 1981, 60, 452–453.
[28] Long FX, Gevert BS. *J. Catal*. 2004, 222, 1–5.
[29] Maher KD, Kirkwood KM, Gray MR, Bressler DC. *Ind. Eng. Chem. Res.* 2008, 47, 5328–5336.
[30] Palanisamy S, Gevert BS. *Appl. Therm. Eng*. 2016, 107, 301–310.
[31] Seifi H, Sadrameli SM. *Appl. Therm. Eng*. 2016, 100, 1102–1110.
[32] Guo Z, Wang S, Yin Q, Xu G, LuoZ, Cen K, Fransson TH. World Renewable Energy Congress (2011). 8–13, May 2011 Sweden BE01, 057:074, 552–559.
[33] Osmont A, Catoire L, Gokalp I, Swihart MT. *Energy Fuels* 2007, 21, 2027–2032.
[34] Carey FA, Sundberg RJ. Kluwer Academic/Plenum Publishers: 4th ed., Springer Science: New York, 2000, pp. 454–457.
[35] Turpeinen E, Sapei E, Uusi-Kyyny P, Keskinen KI, Krause OAI. *Fuel* 2011, 90, 3315–3322.
[36] Kubicka D, Horacek J. *Appl. Catal. A* 2011, 394, 9–17.
[37] Rollmann LD. *J. Catal.* 1977, 46, 243–252.
[38] Priecel P, Kubicka D, Capek L, Bastl Z, Rysanek P. *Appl. Catal. A* 2011, 397, 127–137.
[39] Priecel P, Kubicka D, Capek L, Bastl Z, Rysanek P, Homola F, Rysanek P, Pouzar M. *Catal. Today* 2011, 176, 409–412.
[40] Graca I, Fernandes A, Lopes JM, Ribeiro MF, Laforge S, Magnoux P, Ribeiro FR. *Fuel* 2011, 90, 467–476.
[41] El-Nahas AM, Navarro MV, Simmie JM, Bozzelli JW, Curran HJ, Dooley S, Metcalfe W. *J. Phys. Chem. A* 2007, 111, 3727–3739.
[42] Galuszka J, Chang JR, Amenomiya Y, Seivama T, Tanabe K. *Studies in Surface Science and Catalysis*, Elsevier, 1981, Vol. 7, pp. 529–541.